

# Holocene coral reef carbonate REY geochemistry during the neomorphism from aragonite to calcite: A case study in the South China Sea

Wei Jiang<sup>a</sup>, Yuwen Xiao<sup>a</sup>, Kefu Yu<sup>a,b,\*</sup>, Rui Wang<sup>a</sup>, Shendong Xu<sup>c</sup>, Ning Guo<sup>a</sup>, Tingwu Gu<sup>a</sup>

<sup>a</sup> Guangxi Laboratory on the Study of Coral Reefs in the South China Sea, School of Marine Sciences, Guangxi University, Nanning, China

<sup>b</sup> Southern Marine Sciences and Engineering Guangdong Laboratory (Guangzhou), Guangzhou, China

<sup>c</sup> Key Laboratory of Coastal Zone Environmental Processes and Ecological Remediation, Yantai Institute of Coastal Zone Research, Chinese Academy of Sciences, Yantai, China

## ARTICLE INFO

Editor: Howard Falcon-Lang

### Keywords:

Rare earth element and yttrium  
Coral reef  
Microbialite  
Neomorphism  
Marine carbonate

## ABSTRACT

The geochemistry of rare earth elements and yttrium (REY with Y, REE without Y) in reefal carbonates is increasingly used to investigate both palaeoceanography and modern oceans. Nevertheless, the application of these methods to elucidate climate dynamics of the geologic past is limited by their vulnerability to diagenetic alterations. Given the meteoric transformation of aragonite to calcite, which represents an extremely unfavorable scenario for preserving the original marine signature, we focused on the REY geochemistry of a Holocene coral reef, obtained from Well CK2 in the northern South China Sea, which initiated at ~7.8 ka BP, but ceased to grow vertically at ~3.9 ka BP. The Holocene reefal carbonates have undergone neomorphism, transforming aragonite into calcite in a meteoric environment and enabling a direct comparison of REY distributions between the original aragonite and neomorphic calcite. Despite the preserved REY patterns of stabilized calcite closely mirroring those initially present in surface seawater, the  $\Sigma$ REE contents and Ce anomalies vary significantly, reflecting mixing of REY from reefal microbialites. Despite these disturbances, the  $Nd_N/Yb_N$  and Y/Ho ratios of Holocene reefal carbonates still demonstrate a highly conservative behavior during diagenesis. Our study indicates that the initial REY parameters, such as  $Nd_N/Yb_N$  and Y/Ho ratios, are frequently preserved in Holocene reefal carbonates, thus offering significant support for employing ancient marine limestones as indicators of marine REY geochemistry. Nevertheless, prudence is advised when utilizing  $\Sigma$ REE contents and Ce anomaly.

## 1. Introduction

Modern and ancient marine carbonates incorporate rare earth elements and yttrium (REY with Y, REE without Y) in proportions akin to those observed in ambient seawater (Luo et al., 2021; Saha et al., 2019; Saha et al., 2021; Webb and Kamber, 2000; Webb et al., 2009; Wyndham et al., 2004; Zhao and Jones, 2013). In recent years, the REY proxy in marine carbonates, including scleractinian corals and microbialites, has been used successfully for tracing marine input origins (Falcone et al., 2022; Saha et al., 2018; Saha et al., 2019; Saha et al., 2021; Wei et al., 2023a; Zhao and Zheng, 2014), environmental pollution (Jiang et al., 2017; Nguyen et al., 2013; Xie et al., 2023), and palaeoceanography and paleoclimate (Bi et al., 2019; Della Porta et al., 2015; Jia et al., 2024; Jiang et al., 2019; Kamber et al., 2014; Li et al., 2019; Liu et al., 2022; Tostevin et al., 2016; Zhang and Shields, 2022; Zhao et al., 2021). Although the fidelity and robustness of modern/ancient marine

carbonates REY proxies are empirically established, the efficacy still relies on the direct syngenetic contamination degree of terrigenous detritus and preservation of original REY signals during subsequent diagenesis (Webb et al., 2009).

Direct terrigenous contamination can be identified through the concurrent presence of reduced mobile elements, such as thorium (Th) and zirconium (Zr) (Nothdurft et al., 2004; Webb and Kamber, 2000), and the effects of diagenesis on REY geochemistry of marine carbonates can be evaluated by the geochemical and mineralogical proxies for diagenesis alteration, such as manganese (Mn)/strontium (Sr) ratio and oxygen isotope ( $\delta^{18}O$ ) (Derry et al., 1994; Higgins et al., 2018; Kaufman and Knoll, 1995). Over the last decades, the above methods have been extensively utilized to evaluate the preservation of original seawater REY signature, and most studies verify the consistent conservative behavior of REY in reefal carbonates throughout a variety of diagenetic changes (Jia et al., 2024; Jiang et al., 2019; Li and Jones, 2014; Liu et al.,

\* Corresponding author at: Guangxi Laboratory on the Study of Coral Reefs in the South China Sea, School of Marine Sciences, Guangxi University, Nanning, China.  
E-mail address: [kefuyu@scsio.ac.cn](mailto:kefuyu@scsio.ac.cn) (K. Yu).

2022; Luo et al., 2021; Shen et al., 2023; Webb et al., 2009; Zhao and Jones, 2013). However, the majority of prior studies have centered on the pre-Holocene limestones or dolomites, which have undergone compaction and lithification. Furthermore, despite the inclusion of Holocene data in some studies, the distinctive characteristics of Holocene carbonates might be obscured in the whole core study, due to their relatively scarce data compared to Pleistocene or other geological strata.

In general, except for the dissolution and recrystallization of metastable carbonate minerals, the characteristics of REY in carbonates are expected to maintain stability over geological timescales (Zhong and Mucci, 1995). Therefore, the REY signatures of marine carbonates are always susceptible to modification during the early diagenetic stage, e.g., neomorphism from aragonite to calcite (Tanaka et al., 2003; Webb and Kamber, 2000; Webb et al., 2009), which has been considered as one of the most unfavorable scenarios for preserving the original REY signature (Webb et al., 2009). Despite the transformation of aragonite to calcite can also be found in pre-Holocene stratum, e.g., the Pleistocene scleractinian coral skeletons of Florida (Webb et al., 2009), it is more readily observed in Holocene strata.

Coral reefs are extensively distributed throughout the South China Sea (SCS) (Yu, 2012), which initiated at the late Oligocene or early Miocene (Fan et al., 2020; Li et al., 2023). Well CK2, drilled on an isolated carbonate platform in the SCS (Fig. 1), yielded core recovery rates averaging ~70 %, with most sections exceeding 80 %, thus providing highly suitable research materials dating back to the early Miocene. According to high-precision uranium(U)-series dating, the initiation of Holocene reefal carbonates, measuring 16.7 m in thickness, occurred approximately 7.8 thousand years before present (ka BP), while vertical accretion ceased around 3.9 ka BP (Ma et al., 2021; Qin et al., 2019). Due to the minimal terrigenous influence, the Holocene reefal carbonates present an exceptional opportunity for investigating the response of REY behavior during neomorphism. This study investigates the REY signatures of the Holocene stratum in Well CK2 with an aim to assess the impact of neomorphism from aragonite to calcite on the REY signature of marine carbonates. The findings will contribute towards evaluating

marine carbonates suitability as geochemical archives for environmental studies.

## 2. Geological settings

SCS is one of the largest low-latitude marginal sea on the globe with an area of  $\sim 3.5 \times 10^6$  km<sup>2</sup>, originally formed due to rapid seafloor spreading during the Cenozoic era (Barckhausen and Roeser, 2013). The Xisha Islands (17°07'-15°43'N, 111°11'-112°54'E) constitute a cluster of atolls located on an elevated submarine plateau in the northwestern SCS, encompassed by seawater at depths exceeding 1 km. The Xisha Islands exhibit a tropical monsoon climate, characterized by an annual precipitation ranging from 1300 to 2000 mm, an average seawater surface temperature ranging from 22 to 30 °C, and near-surface salinity levels ranging from 33.14 to 34.24 ‰. The carbonate platforms surrounding the Xisha Islands exhibited extensive development, with reef and platform growth displaying relatively high activity levels during the middle Miocene, decreasing significantly during the late Miocene, and ranging from moderate to active during the Pliocene and Pleistocene periods (Fan et al., 2020; Shao et al., 2017; Wu et al., 2014). Well CK2, drilled in 2013 on Chenhang Island (16°27' N, 111°43' E) in the southeast of the Yongle Atoll, comprises a Cenozoic carbonate succession extending to a depth of 873.55 m, along with the volcanoclastic basement reaching a depth of 928.75 m. Considering the relative stability of neotectonic activities in the study area, as well as the fact that the reef flat of modern coral reefs in the SCS is predominantly situated at low tide height, and with Well CK2's borehole positioned approximately 2.9 m above this modern reef flat, it can be inferred that originally, the top of Well CK2 was located around 13.8 m below the low tide level of present-day sea (Qin et al., 2019).

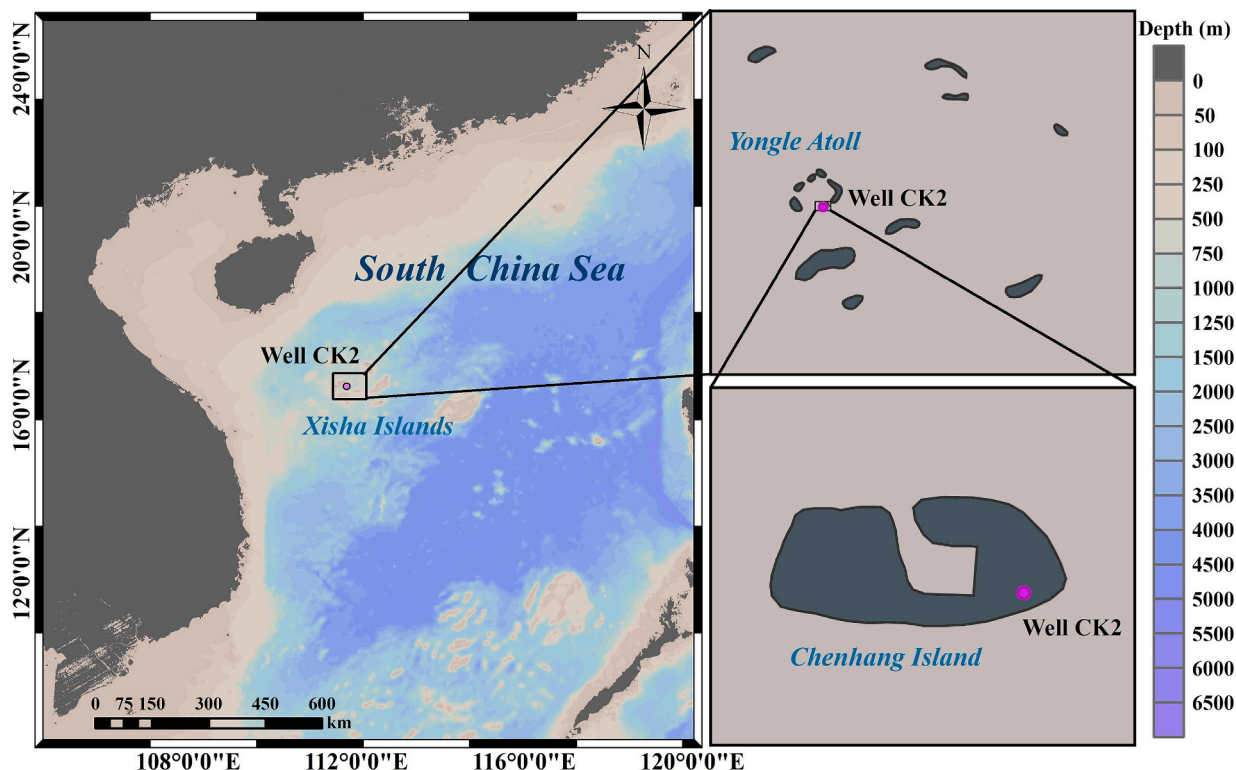


Fig. 1. Locality map of Well CK2 on the Chenhang Island of the Yongxing Atoll in the Xisha Islands, northern SCS.

### 3. Material and methods

#### 3.1. Core chronology

Based on Qin et al. (2019) and Ma et al. (2021), the Pleistocene/Holocene boundary of Well CK2 was determined to be located 16.7 m below the drilling surface. The upper 16.7 m section of the core was sampled to obtain 18 well-preserved *Acropora* spp. Specimens (Fig. S1 in the Supplemental Materials) to establish a comprehensive chronostratigraphy of the Holocene coral reef. The samples were cleaned and sectioned to eliminate any surface impurities, e.g., drilling mud and loose sediments, subjected to ultrasonic oscillation in distilled water for debris particle removal, dried at 50 °C, and finally sealed in plastic bags. The U-series ages of the samples were determined by the Nu plasma multicollector inductively coupled plasma mass spectrometer at the University of Queensland, enabling precise determination of isotopic ratios and elemental concentrations with an accuracy within  $\pm 1\text{--}2\%$  ( $2\sigma$ ) (Clark et al., 2014). The U-thorium (Th) isotopic data and  $^{230}\text{Th}$  dates can be seen in supporting information Table S1 and 11 samples were selected to establish the age framework based on the order from the youngest to the oldest in this study after removing age reversed samples (Fig. 2). The determination of age framework in details is provided in Ma et al. (2021).

#### 3.2. Lithology and mineralogy

The mineral species and mass percentages were determined through the utilization of X'Pert PRO diffractometer according to  $2\theta$  angle and spectral peak intensity (Fig. S2). The lithological characteristics and mineralogy of Well CK2 were analyzed by conducting microscopic observations on about 300 thin sections using a polarizing microscope. The results indicate that the core from Well CK2, spanning from 16.7 to 0 m, predominantly consists of a coral debris mixture containing aragonite, high-Mg calcite and low-Mg calcite (Fig. 3). The entire core is comprised of identical constituent groups, predominantly coral (*Acropora* spp., accounting for 59.35 %) and fragments of coralline algae. The observation of coral, originally composed of aragonite, undergoing the aragonite-calcite transformation provided evidence for the existence of the aragonite-calcite transformation (Fig. S3).

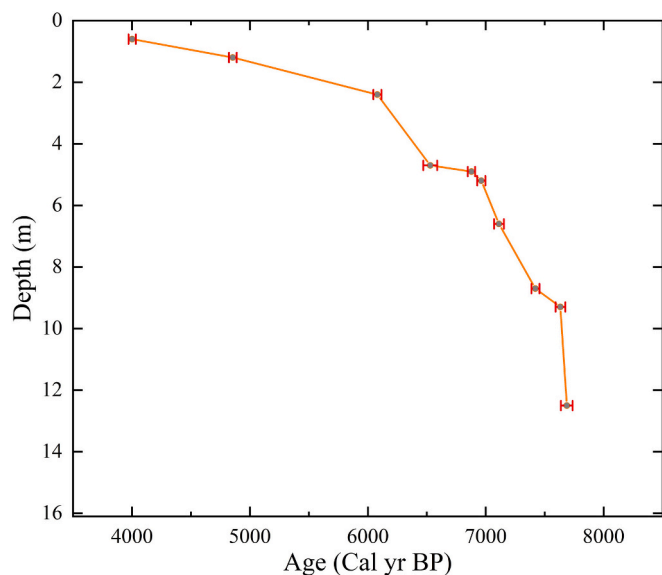


Fig. 2. Calibrated U-Th age framework of the Holocene section of Well CK2 core.

#### 3.3. Geochemical analysis

Geochemical analyses of the samples were conducted at the Guangxi University, China. 14 carbonate powder samples from relatively well-preserved corals collected at an interval of  $\sim 1$  m from the uppermost  $\sim 16.7$  m section of Well CK2. The  $\delta^{18}\text{O}$  analysis was conducted using a Finnigan MAT-253 stable isotope mass spectrometer coupled with a Fairbanks carbonate preparation device. The isotopic ratios were presented in the per mil (‰) convention and normalized to the V-PDB in accordance with the GBW04405 standard. Repeated measurements of this standard produced a standard deviation of 0.08 ‰ for  $\delta^{18}\text{O}$ . The carbonate samples were processed and analyzed for elemental compositions using standard techniques with an inductively coupled plasma emission mass spectrometer. The isotopes of REY ( $^{89}\text{Y}$ ,  $^{139}\text{La}$ ,  $^{140}\text{Ce}$ ,  $^{141}\text{Pr}$ ,  $^{146}\text{Nd}$ ,  $^{149}\text{Sm}$ ,  $^{153}\text{Eu}$ ,  $^{159}\text{Tb}$ ,  $^{160}\text{Gd}$ ,  $^{161}\text{Dy}$ ,  $^{165}\text{Ho}$ ,  $^{167}\text{Er}$ ,  $^{169}\text{Tm}$ ,  $^{172}\text{Yb}$ , and  $^{175}\text{Lu}$ ), along with other trace metals ( $^{31}\text{P}$ ,  $^{55}\text{Mn}$ ,  $^{57}\text{Fe}$ ,  $^{88}\text{Sr}$ , and  $^{92}\text{Zr}$ ), exhibit distinctive signals. The levels of barium oxide and rare earth oxide were determined by analyzing pure elemental solutions, with appropriate corrections made for any potential interferences. The concentrations of phosphorus pentoxide ( $\text{P}_2\text{O}_5$ ) and ferric oxide ( $\text{Fe}_2\text{O}_3$ ) applied in this study were determined based on the P and Fe concentrations. The analyzed data were assessed for accuracy and precision through a comprehensive quality assurance and quality control program, which encompassed the utilization of reagent blanks, duplicate tests, and certified geochemical reference materials (GBW07129, GBW07133, GBW07135) with deviations below 5 %. The detailed procedures were described in Xu et al. (2019) and Jiang et al. (2019).

#### 3.4. Interpretations for proxies

The distribution patterns of REY in Holocene carbonate samples are demonstrated by normalizing the REY against the standard Post-Archean Average Shale (PAAS) (McLennan, 1989) and plotting them on a logarithmic scale as a function of the atomic numbers of the respective elements. The  $X_N$  represent the PAAS-normalized concentrations of X, and the  $\text{Nd}_N/\text{Tb}_N$  ratio is used to represent light REE (LREE)/heavy REE (HREE). The Y/Ho mass ratios are computed without undergoing any form of normalization. Ce anomaly ( $\text{Ce}/\text{Ce}^* = \text{Ce}/(\text{Pr}^2/\text{Nd})$ ) and Eu anomaly ( $\text{Eu}/\text{Eu}^* = \text{Eu} \times 2/(\text{Sm} + \text{Gd})$ ) are calculated by geometrically/linear extrapolating Pr and Nd, Sm and Gd, respectively.

## 4. Results

#### 4.1. Lithofacies, depositional facies and mineralogy

The uppermost 16.7 m interval of Well CK2 consists predominantly of unconsolidated coarse sediments, comprising coral, large benthic foraminifera, mollusks, and coralline algae. The particle size distribution is dispersed and the frequency of the particle size is not well-defined or abrupt, indicating a shallow seawater environment characterized by moderate to high energy levels. The Holocene sedimentary environment of Well CK2 was characterized by unconsolidated bioclastic limestone and coral debris.

The upper 16.7 m section of Well CK2 can be classified into three units based on mineral compositions (Fig. 3). Unit I (0– $\sim 2$  m) primarily consists of aragonite, with minor occurrences of high-Mg calcite. In Unit II ( $\sim 2$ – $\sim 10$  m), the majority of primary aragonite has undergone transformation to high-Mg calcite within this unit. Unit III ( $\sim 10$ – $16.7$  m) is characterized by predominant low-Mg calcite, accompanied by minor amounts of aragonite or high-Mg calcite.

#### 4.2. Elemental and isotopic geochemical characteristics

The REY proxies of the Well CK2 above 16.7 m are presented in Fig. 3. The Ce anomaly, Eu anomaly and  $\text{Nd}_N/\text{Yb}_N$  ratios do not exhibit any discernible trends except several extremes, with the respective

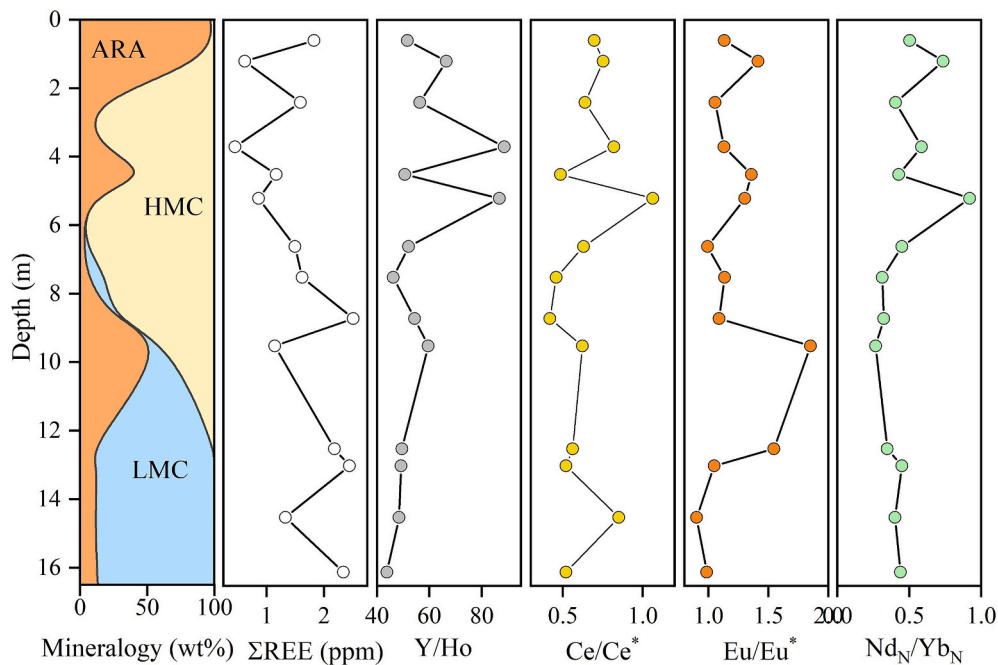


Fig. 3. Mineral compositions (ARA: aragonite; HMC: high-Mg calcite; LMC: low-Mg calcite) and REY profiles from the top ~16.7 m section of Well CK2 core.

ranges of 0.42–1.06 (average  $\pm$  standard deviation (SD):  $0.65 \pm 0.17$ ), 0.90–1.85 (average  $\pm$  SD:  $1.21 \pm 0.25$ ), and 0.27–0.92 (average  $\pm$  SD:  $0.47 \pm 0.17$ ). A visible secular variation trend can be observed in the sequence of  $\Sigma$ REE content and Y/Ho ratios, with the respective ranges of 0.45–2.50 ppm (average  $\pm$  SD:  $1.54 \pm 0.64$  ppm) and 43.70–88.58 (average  $\pm$  SD:  $57.37 \pm 13.53$ ). All the carbonate samples have typical seawater REY patterns, characterized by the depletion in LREE compared to the HREE, superchondritic Y/Ho ratios, a slight positive Eu anomaly, and a negative Ce anomaly, as observed in Fig. 4.

As a typical detrital element, Zr ranges from 0.26 to 1.99 ppm, with an average of  $0.86 \pm 0.42$  ppm. The Mn and Sr have the ranges of 4.07–83.62 ppm (average  $\pm$  SD:  $30.98 \pm 22.53$  ppm) and 0.52–9.25 % (average  $\pm$  SD:  $1.41 \pm 2.18$  %), respectively. The  $P_2O_5$  and  $Fe_2O_3$  have the ranges of 0.04–0.15 % (average  $\pm$  SD:  $0.08 \pm 0.03$  %) and 0.06–0.33 % (average  $\pm$  SD:  $0.17 \pm 0.08$  %), respectively. The  $\delta^{18}O$  values range from  $-5.06$  to  $-2.10$  ‰ (average  $\pm$  SD:  $-3.43 \pm 0.77$  ‰) throughout the uppermost 16.7 m interval of Well CK2.

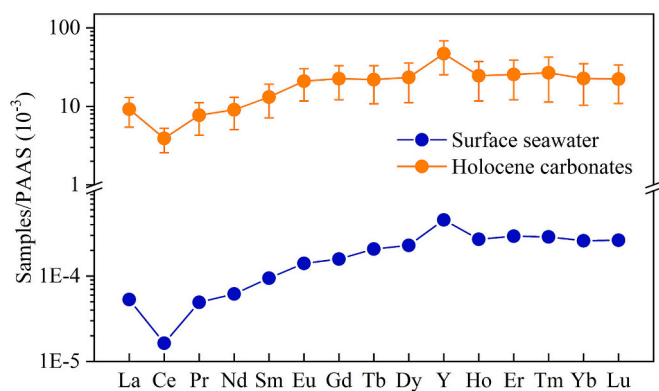


Fig. 4. The PAAS-normalized REY patterns of surface seawater samples from SCS and carbonates in the Well CK2 (0–16.7 m). The REY curve represented the average  $\pm$  standard deviation. The data of SCS seawaters is from Alibo and Nozaki (2000).

## 5. Discussion

### 5.1. Impacts of contaminations and diagenesis

The exogenous sources, characterized by elevated REY contents and distinctive REY patterns, may overprint the carbonate REY signals (Nothdurft et al., 2004). This isolated carbonate system contained minimal fine siliciclastic particulates, which is consistent with the low  $\Sigma$ REE levels observed. In addition, the non-carbonate contaminations were always evaluated based on several criteria, including Zr for detritus, Fe for Fe-Mn(oxyhydr)oxides, and P for phosphates (Nothdurft et al., 2004; Zhao et al., 2022). The Zr, abundant in shale ( $\sim 210$  ppm), occurs in concentrations  $\sim 0.86$  ppm in carbonate samples, indicating  $<1$  % shale contamination. Despite the potential influences from the very small amounts of shale with high REY concentrations on REY patterns, this possibility has been dismissed due to the lack of significant correlation between  $\Sigma$ REE and Zr (Fig. 5). Likewise, the low  $Fe_2O_3$  concentrations ( $<0.35$  %) and absence of correlation observed in the plot depicting  $Fe_2O_3$  concentrations against REY parameters (Fig. S4) suggests that Fe-Mn(oxyhydr)oxides do not exert a significant control over REY patterns. The  $P_2O_5$  concentrations ( $<0.2$  %) exhibit no significant correlation with the Y/Ho ratios and  $Nd_N/Yb_N$ , but they do display a strong correlation with  $\Sigma$ REE and Ce anomalies (Fig. 6). This suggests that phosphates, which can disproportionately incorporate REY and are susceptible to diagenesis alteration (German and Elderfield, 1990; Reynard et al., 1999), account for the observed effects. Therefore, while the  $\Sigma$ REE and Ce anomalies of carbonate samples may not accurately reflect the primary signal, it is expected that the signals of Y/Ho ratios and  $Nd_N/Yb_N$  ratios may be well-preserved in these samples.

The diagenetic processes involve the early marine diagenesis, chemical exchange between the solid phase and pore-fluid, transforming metastable aragonite and high-Mg calcite into low-Mg calcite rocks (Higgins et al., 2018). The sedimentary composition of the area is predominantly loose, with a notable lack of strong cementation. Only acicular aragonite cement can be observed within the interstices of certain coral fragments, which is commonly believed to have formed during the quasi-simultaneous period in a marine environment and likely shares similar REE chemical characteristics with seawater (Sholkovitz and Shen, 1995; Webb et al., 2009). Meanwhile, early

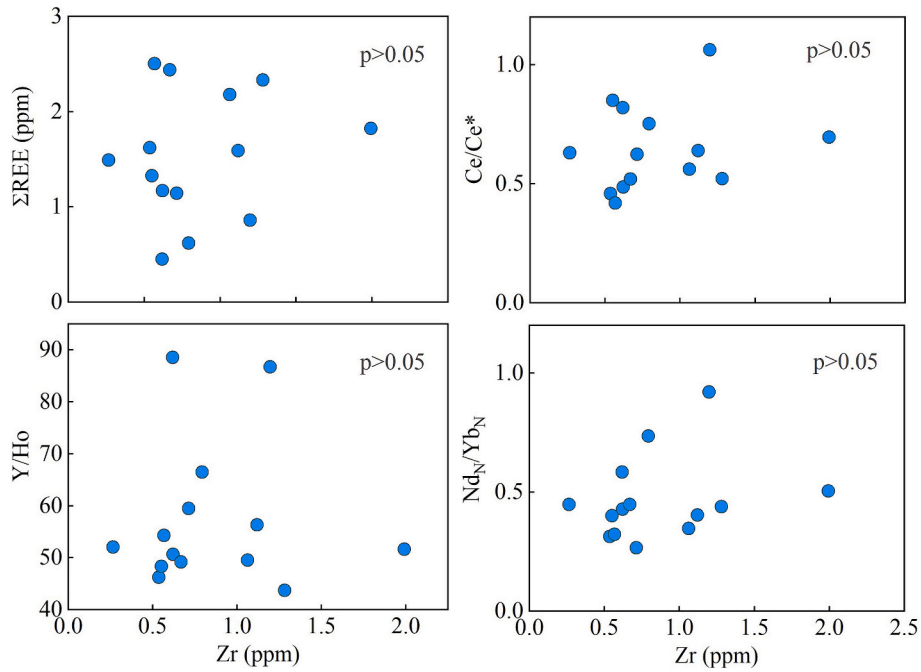


Fig. 5. Co-variation plots of REY parameters against Zr in the top ~16.7 m section of Well CK2 core.

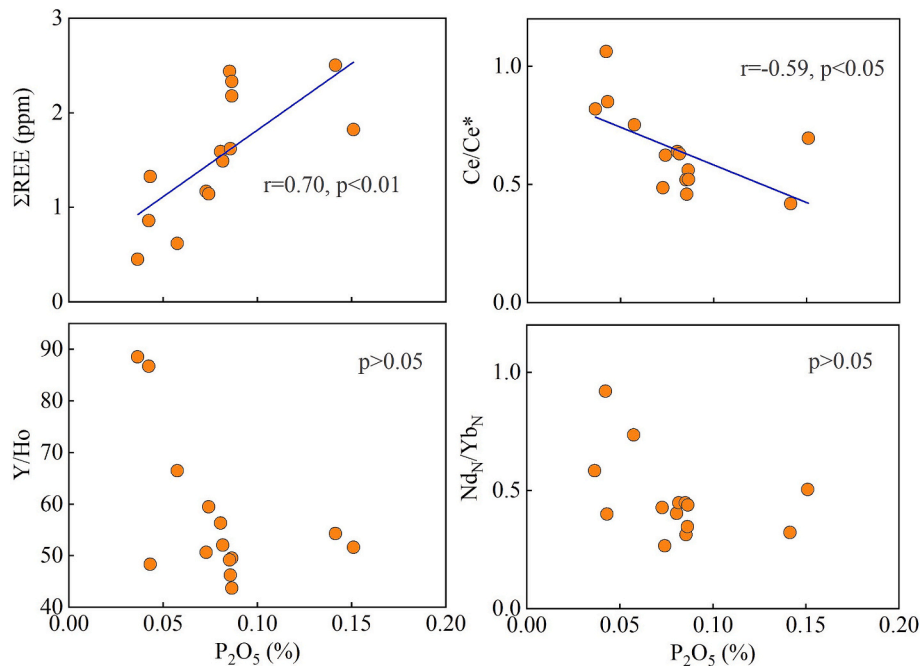


Fig. 6. Co-variation plots of REY parameters against  $P_2O_5$  in the top ~16.7 m section of Well CK2 core.

marine diagenesis has been reported not to invalidate the utility of shallow-marine carbonates as proxies for the seawater chemistry (Wei and Zhang, 2024). Therefore early marine diagenesis can not affect the behavior of REY. The mineralogy (%) exhibits a poor correlation with the REY parameters (Fig. 7), indicating that the stabilization of the REY patterns of neomorphic calcites during the diagenetic processes (Frimmel, 2009; Webb and Kamber, 2000; Webb et al., 2009). From the view of geochemistry, the majority of diagenetic fluids typically exhibit low Sr concentrations and high Mn concentrations (Kaufman and Knoll, 1995). Additionally, meteoric fluids are characterized by isotopically depleted  $\delta^{18}O$  values (Derry et al., 1994). The commonly employed

thresholds for assessing the preservation of primary signals are about 1 for Mn/Sr ratios and  $-10\text{‰}$  for  $\delta^{18}O$  values (Higgins et al., 2018). In the carbonate samples, the  $\delta^{18}O$  results varied between  $-5.06\text{‰}$  and  $-2.10\text{‰}$ , with an average of  $-3.43\text{‰}$ , all surpassing the lower limit of  $-10\text{‰}$ . Meanwhile, the  $\delta^{18}O$  values exhibit weak correlations with both the  $\Sigma\text{REE}$  and Y/Ho ratios across various sedimentary facies. Likewise, the Mn/Sr ratios ranged from 0.0005 to 0.0141, with an average value of 0.0036, significantly below the threshold of 1. The correlation between the Mn/Sr ratios and Y/Ho ratios is found to be poor, whereas a significant association between the Mn/Sr ratios and  $\Sigma\text{REE}$  can be observed (Fig. 8).

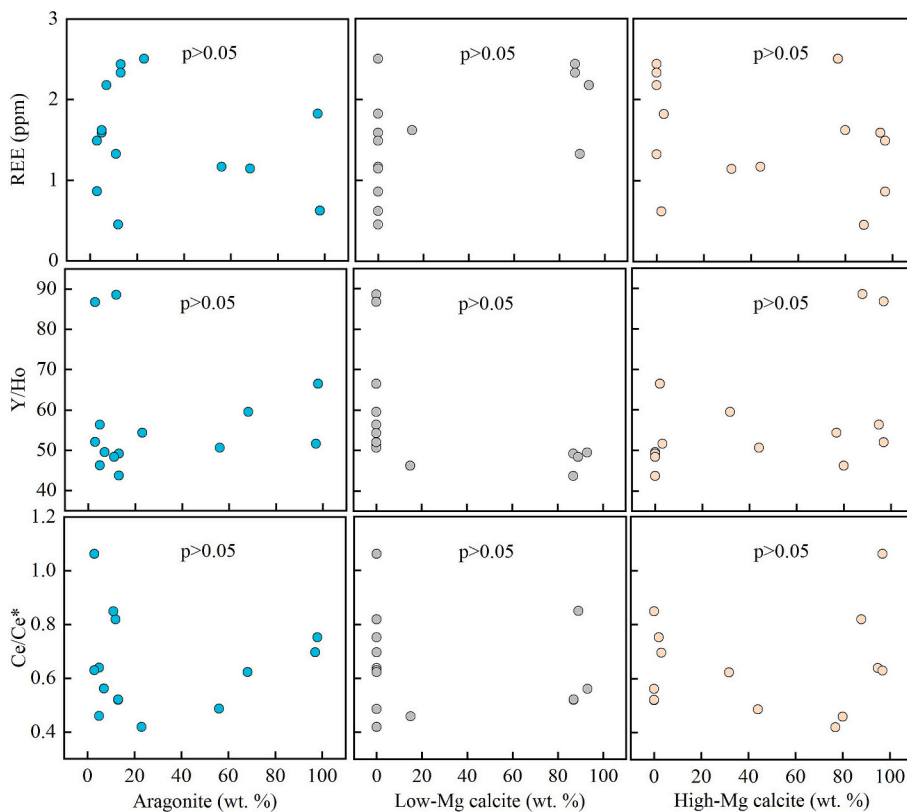


Fig. 7. Co-variation plots of REY parameters against mineral compositions in the top  $\sim 16.7$  m section of Well CK2 core.

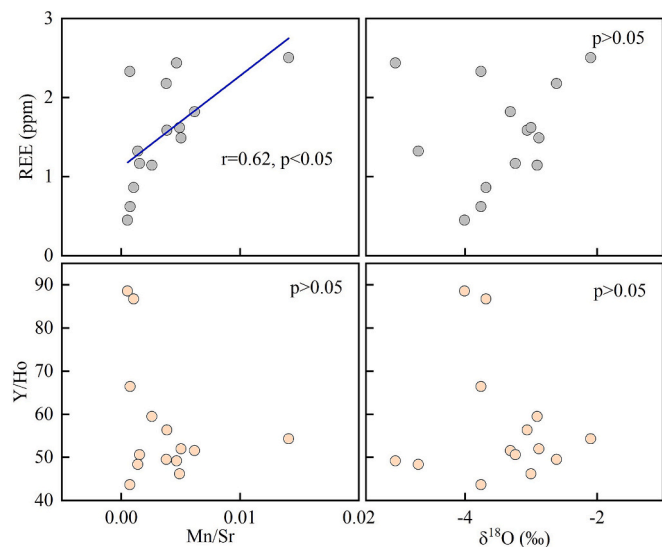


Fig. 8. Co-variation plots of REY parameters against Mn/Sr ratios and  $\delta^{18}\text{O}$  values in the top  $\sim 16.7$  m section of Well CK2 core.

Considering the significant correlations among Mn/Sr ratios,  $\text{P}_2\text{O}_5$ , and  $\Sigma\text{REE}$  (Figs. 6 and 8), we inferred that the phosphates were affected by diagenetic alteration, resulted in the variations in  $\Sigma\text{REE}$  (German and Elderfield, 1990; Reynard et al., 1999). In fact, there are a certain amount of phosphates, such as microbialites containing phosphate, fish teeth and bones, crustacea, lingulata etc., in the Holocene sediments, and P could also be bound to the carbonate grains (Dodd et al., 2021; Monbet et al., 2007; Ning et al., 2020). Furthermore, it is plausible that the recrystallization process of apatite contributes to the reenrichment of REY (Liu et al., 2023). The weak correlation between  $\text{P}_2\text{O}_5$  and Ce/

Ce\* is likely transmitted from the strong negative correlation observed between  $\Sigma\text{REE}$  and Ce/Ce\* ( $r = 0.67$ ,  $p < 0.01$ ).

## 5.2. REE behavior during neomorphism

In comparison to the overlying aragonite, the neomorphic calcite seems to exhibit distinctive characteristics (Fig. 3), including an increased  $\Sigma\text{REE}$  concentration, a heightened negative Ce anomaly, and an augmented depletion of light REE (lower  $\text{Nd}_\text{N}/\text{Yb}_\text{N}$  ratios), aligning with the REE parameters observed in Pleistocene scleractinian coral skeletons during meteoric diagenesis (Webb et al., 2009). Despite the weak correlation between  $\Sigma\text{REE}$  and mineralogy, a visible increase in REE concentration is observed from aragonite to calcite (Fig. 3). The majority of REY seem to be preserved through neomorphism, and the neomorphic calcite samples exhibit higher REY levels compared to aragonite (Fig. 3), albeit with predominantly similar PAAS-normalized patterns (Fig. 4). One hand, Webb et al. (2009) suggested that: (i) during the dissolution of calcite, the REY released are promptly sequestered by the adjacent deposited calcite; and (ii) upon the complete dissolution of marine limestone, the REY released will subsequently be sequestered by the newly formed calcite cement, leading to a slight enrichment of these elements within the new calcite. On the other hand, in comparison to the interactions between fluids and aragonite, the REY exhibit high distribution coefficients between calcite and diagenetic fluids, along with a strong tendency to bind to the surfaces of carbonate structures, which may result in the sequestration of REY during neomorphism (Lakshtanov and Stipp, 2004; Stipp et al., 2003). In general, the empirical distribution coefficients of REY between aragonite coral skeletons and fluids typically fall within the range of 1 to 5 (Akagi et al., 2004; Sholkovitz and Shen, 1995; Wyndham et al., 2004). Despite the empirical and experimental evidences are contradictory concerning calcite (Scherer and Seitz, 1980; Tanaka and Kawabe, 2006; Webb and Kamber, 2000; Zhong and Mucci, 1995), the REY partition coefficients between fluids and calcite exhibit significantly higher values (e.g., 2.5 to

10 (Terakado and Masuda, 1988), ~100 (Scherer and Seitz, 1980), ~300 (Toyama and Terakado (2019); Webb and Kamber, 2000) compared to those observed between fluids and aragonite in equivalent experiments. Considering that the vast majority of samples, initially composed of aragonite, have now transformed into high-Mg calcite and low-Mg calcite, it is likely that the relatively higher  $\Sigma$ REE content in these carbonates can be attributed to their diagenetic processes. Despite the significant changes in  $\Sigma$ REE concentrations, the calcite REY patterns were retained largely intact due to proportionally scavenging of REY during the neomorphic calcite precipitation (Stüpp et al., 2003) and the low levels of fluid REY concentrations.

Direct contamination by particulate matter and the dissolution of microbialites can also increase REY concentration (Cabiocch et al., 2006; Webb et al., 2009; Webb and Kamber, 2000). Overall, the selective uptake of LREE by particulate matter could explain the nearly flat distribution and the minimal negative Ce anomaly (Webb et al., 2009). Obviously, the relatively low  $Nd_N/Yb_N$  ratios and well-developed negative Ce anomalies of neomorphic calcites (Fig. 3) ruled out the possibility of particulate matters. Reefal microbialites represent the advanced stage of encrustation on deceased coral colonies or, more commonly, on related encrusting organisms, thereby forming surface crusts (Camoin et al., 2006). Microbialites are commonly found within cavities of coral frameworks (Heindel et al., 2012) and have been demonstrated to contemporaneously develop alongside reef frameworks or slightly postdate associated corals by a few centuries (Webb and Jell, 2006; Westphal et al., 2010). As a feature of rapid sea-level rise and abrupt climatic changes, microbialites have been identified widespread development in the Holocene and modern reefs in the South China Sea (Gong et al., 2017; Heindel et al., 2012; Shen and Wang, 2008; Teng and Shen, 2008; Yang et al., 2023; Zhang et al., 2022). Reefal microbialites contain REY in higher concentration than corals (Webb and Kamber, 2000), thus enhancing testability to facilitate precise value assessment and providing robust seawater REY proxies for ancient reefs and carbonate platforms (Kamber and Webb, 2001; Kamber et al., 2014; Nothdurft et al., 2004; Olivier and Boyet, 2006). The dissolution of microbialite would not only result in an increased concentration of REY in pore fluids but also introduce an increasing negative Ce anomaly (Cabiocch et al., 2006; Webb and Kamber, 2000). Therefore, we hypothesize that the microbialites, which exhibited sensitivity to diagenetic alteration, may account for the strong associations observed between  $\Sigma$ REE and Ce anomaly ( $r = -0.67$ ,  $p < 0.01$ ), as well as the correlation between  $\Sigma$ REE and Mn/Sr ratio (Fig. 8). It's worth noting that the growth of microbialites is typically succeeded by the formation of phosphatic-iron-manganese crusts, with phosphatic films frequently interlayering with microbial laminae on the external surfaces of the crusts and coating borings within both the microbialite and underlying red algal-foraminiferal encrustations (Camoin et al., 2006). Therefore, the microbialites containing phosphate might explain the significant correlations among  $P_2O_5$ ,  $\Sigma$ REE and Ce anomaly (Fig. 6 and S2).

The reduction in LREE depletion in carbonates is thought to result from several factors, including the influences of terrigenous inputs (Nothdurft et al., 2004; Webb et al., 2009), variations in depositional settings (Kamber and Webb, 2001), and/or differences in diagenetic histories (Mazumdar et al., 2003). The  $Nd_N/Yb_N$  ratios, however, exhibit no discernible variations with respect to the diagenetic indices and mineral compositions (Fig. S5), implying that diagenesis exerted negligible influence on the depletion of LREEs. Salas-Saavedra et al. (2022) reported that reefal microbialite-hosted REY distributions ( $Nd_N/Yb_N$  and Y/Ho ratio) were consistent with shallow oxygenated seawater, and might provide high-quality proxies for ambient water quality. However, Mazumdar et al. (2003) proposed that the basicity of pore fluids in both the unsaturated and saturated zones, which increases due to organic matter degradation, facilitates the incorporation of HREE into the carbonate lattice. The transformation of aragonite and/or high-Mg calcite into low-Mg calcite potentially occurred within a mixed freshwater and seawater environment (MacNeil and Jones, 2003). Nevertheless, the

limited depletion of LREE and the absence of any observed correlation between  $Nd_N/Yb_N$  ratios and diagenetic indices in carbonates may suggest negligible effects of meteoric processes throughout the transformation of aragonite and calcite. Actually, meteoric diagenesis does not invariably obscure the geochemical signature of primary carbonate minerals (Wei et al., 2023b). In this study, the  $Nd_N/Yb_N$  and Y/Ho ratios, which demonstrate limited correlations with both diagenetic alteration and non-carbonate contamination indexes, should be preserved as the primary REY signature during the neomorphism processes.

### 5.3. Interpretation of REY patterns

The Holocene carbonate REY patterns are characterized by (1) positive La anomalies, (2) negative Ce anomalies, (3) LREE depletion relative to HREE, and (4) superchondritic Y/Ho molar ratios (Fig. 4), similar to those found in other Quaternary marine carbonates (Jia et al., 2024; Luo et al., 2021; Webb and Kamber, 2000; Webb et al., 2009) and modern seawater in the South China Sea (Alibo and Nozaki, 1999, 2000). The Eu anomalies of most samples vary within the typical range of seawater (0.9–1.5) (Tostevin et al., 2016), and exhibit no clear trend. However, subtle distinctions exist among the REY patterns of the three units in terms of their Ce anomalies,  $Nd_N/Yb_N$  and Y/Ho ratios. All the Holocene carbonate samples exhibited negative Ce anomalies (Fig. 3). Tanaka et al. (2003) suggested that the Ce/Ce\* of carbonates might indicate the depth of the seawater where the initial diagenetic processes occurred. The Ce/Ce\* ratios of carbonates are consistent with those of modern surface seawater (Alibo and Nozaki, 2000), suggesting the presence of an oxygen-rich environment during their formation. The predominant process responsible for negative Ce anomalies in seawater is the oxidation of dissolved Ce(III) to particulate Ce(IV), associated with redox. Despite the possible influence of phosphates, the Holocene carbonate samples still exhibit the oxidation characteristics inherent to the original surface seawater.

Excluding the potential influences of mineralogy (Webb et al., 2009) and diagenesis (Azmy et al., 2011; Tanaka et al., 2003) on REY in carbonates, the variations in the  $Nd_N/Yb_N$  and Y/Ho ratios should primarily reflect the composition of the seawater during carbonate formation (Azmy et al., 2011). The observed variations in the  $Nd_N/Yb_N$  ratios of carbonates are likely attributed to fluctuations in the REY composition of seawater, as carbonates solely acquire REY from the surrounding seawater. The  $Nd_N/Yb_N$  ratios exhibit an increasing trend with depth in contemporary seawater (Alibo and Nozaki, 1999, 2000). Nonetheless, the gradual rise in  $Nd_N/Yb_N$  ratios with depth cannot be exclusively linked to differences in the initial depositional settings, since all the carbonates were formed in shallow marine environments. As a result, the recorded increase in  $Nd_N/Yb_N$  ratios with depth (Fig. 3) could indicate a long-term shift in the REY composition of seawater. The  $Nd_N/Yb_N$  ratio, indicative of LREE depletion, is consistently attributed to the preferential affinity of LREE towards scavenging processes prevalent in seawater (Wyndham et al., 2004). However, many factors including the continental weathering inputs (Akagi et al., 2004; Caetano-Filho et al., 2018; Saha et al., 2019; Wyndham et al., 2004) and mineralization and desorption processes occurring on the biogenic particles (Li et al., 2019) may influence the LREE depletion of seawater. Compared with modern seawaters in the SCS, the LREE depletion of carbonate samples are all within the range of surface seawater (Alibo and Nozaki, 2000). Considering the narrow range (0.27–0.92), the  $Nd_N/Yb_N$  ratios of Holocene carbonate might represent the secular change of LREE depletion of surface seawater in the open ocean, rather than being influenced by other impact factors.

Nozaki et al. (1997) proposed that Y and Ho exhibit relatively short residence times in the marine environment, with their fractionation primarily governed by scavenging processes associated with the complexation of Y and Ho on particles. The Y/Ho ratios are highest in open ocean settings, exceeding 44; they are intermediate in restricted marine environments, ranging from 25 to 44; and lowest in freshwater

systems and shale deposits, below 25 (Nozaki et al., 1997; Tostevin et al., 2016). The Y/Ho ratios of all samples, which are consistent with a seawater origin (Alibo and Nozaki, 2000), exhibit depth-dependent variations (Fig. 3). Overall, the Y/Ho ratios in surface seawater are primarily influenced by continental inputs and local oceanographic processes (Mazumdar et al., 2003). The Y/Ho ratios of Holocene carbonate samples fall between those of open ocean water and shale/freshwater (Nozaki et al., 1997; Tostevin et al., 2016), indicating a blend of terrigenous materials and oceanic seawater. In fact, the reef carbonate Y/Ho ratio has been utilized as reliable proxy for enhanced terrigenous inputs in the South China Sea (Jia et al., 2024). According to Fig. 3, our findings indicate an overall declining trend in terrigenous inputs over time.

## 6. Conclusions

We have conducted a REY analysis of a Holocene reef core in the Xisha Islands, northern SCS. Our findings suggest that Holocene reef carbonates preserve certain original REY signatures, such as  $Nd_N/Yb_N$  and Y/Ho ratios, derived from the surface seawater in which they formed, provided that they experience minimal terrigenous input and diagenetic alterations. Despite the REY parameters and patterns are consistent with those observed in other Holocene carbonate cores/corals in the SCS, the  $\Sigma$ REE contents should be impacted by both neomorphism and phosphates. In addition, the Ce anomaly variations were associated with the phosphates. We inferred that the reefal microbialites, which exhibited sensitivity to diagenetic alteration, might be responsible for the variations of  $\Sigma$ REE contents and Ce anomaly during the neomorphism. Hence, we postulate that the  $Nd_N/Yb_N$  and Y/Ho ratios of Holocene reef carbonates can serve as crucial indicators for understanding paleoceanography. However, caution is necessary when using  $\Sigma$ REE contents and Ce anomaly for analysis.

## CRedit authorship contribution statement

**Wei Jiang:** Writing – review & editing, Writing – original draft, Visualization, Resources, Methodology, Investigation, Formal analysis, Data curation, Conceptualization. **Yuwen Xiao:** Writing – review & editing, Investigation, Formal analysis. **Kefu Yu:** Supervision, Resources, Investigation, Funding acquisition, Data curation, Conceptualization. **Rui Wang:** Investigation, Data curation. **Shendong Xu:** Investigation, Data curation. **Ning Guo:** Writing – review & editing. **Tingwu Gu:** Writing – review & editing.

## Declaration of competing interest

The authors declare that they have no known competing financial interests or personal relationships that could have appeared to influence the work reported in this paper.

## Acknowledgments

This work was financially supported by the National Natural Science Foundation of China (Grant Nos. 42030502, 41976059 and 42090041), National Key Research and Development Program of China (Grant No. 2023YFF0804801) and the major talent project of Guangxi Zhuang Autonomous Region (GXR-1BGQ2424020). The authors thank Dr. Tianlai Fan, Dr. Siqi Wu, Yeman Qin, Yifang Ma from Guangxi University for their work and helpful advices. Thanks are due to the responsible editor and anonymous reviewers for their critical reviews, which greatly improved our paper.

## Appendix A. Supplementary data

Supplementary data to this article can be found online at <https://doi.org/10.1016/j.palaeo.2025.112835>.

## Data availability

Data will be made available on request.

## References

- Akagi, T., Hashimoto, Y., Fu, F., Tsuno, H., Tao, H., Nakano, Y., 2004. Variation of the distribution coefficients of rare earth elements in modern coral-lattices: species and site dependencies. *Geochim. Cosmochim. Acta* 68, 2265–2273.
- Alibo, D.S., Nozaki, Y., 1999. Rare earth elements in seawater: particle association, shale-normalization, and Ce oxidation. *Geochim. Cosmochim. Acta* 63, 363–372.
- Alibo, D.S., Nozaki, Y., 2000. Dissolved rare earth elements in the South China Sea: Geochemical characterization of the water masses. *J. Geophys. Res. Atmos.* 105, 28771–28784.
- Azmy, K., Brand, U., Sylvester, P., Gleeson, S.A., Logan, A., Bitner, M.A., 2011. Biogenic and abiogenic low-Mg calcite (bLMC and aLMC): Evaluation of seawater-REE composition, water masses and carbonate diagenesis. *Chem. Geol.* 280, 180–190.
- Barckhausen, U., Roeser, H.A., 2013. Seafloor Spreading Anomalies in the South China Sea Revisited, Continent-Ocean Interactions within East Asian marginal Seas. *Am. Geophys. Union* 121–125.
- Bi, D., Zhai, S., Zhang, D., Xiu, C., Liu, X., Liu, X., Jiang, L., Zhang, A., 2019. Geochemical Characteristics of the Trace and rare Earth elements in Reef Carbonates from the Xisha Islands (South China Sea): Implications for Sediment Provenance and Paleoenvironment. *J. Ocean Univ. China* 18, 1291–1301.
- Cabioch, G., Camoin, G., Webb, G.E., Le Cornec, F., Garcia Molina, M., Pierre, C., Joachimski, M.M., 2006. Contribution of microbialites to the development of coral reefs during the last deglacial period: Case study from Vanuatu (South-West Pacific). *Sediment. Geol.* 185, 297–318.
- Caetano-Filho, S., Paula-Santos, G.M., Dias-Brito, D., 2018. Carbonate REE + Y signatures from the restricted early marine phase of South Atlantic Ocean (late Aptian – Albian): the influence of early anoxic diagenesis on shale-normalized REE + Y patterns of ancient carbonate rocks. *Palaeogeogr. Palaeoclimatol. Palaeoecol.* 500, 69–83.
- Camoin, G., Cabioch, G., Eisenhauer, A., Braga, J.C., Hamelin, B., Lericolais, G., 2006. Environmental significance of microbialites in reef environments during the last deglaciation. *Sediment. Geol.* 185, 277–295.
- Clark, T.R., Zhao, J.-X., Roff, G., Feng, Y.-X., Done, T.J., Nothdurft, L.D., Pandolfi, J.M., 2014. Discerning the timing and cause of historical mortality events in modern Porites from the Great Barrier Reef. *Geochim. Cosmochim. Acta* 138, 57–80.
- Della Porta, G., Webb, G.E., McDonald, I., 2015. REE patterns of microbial carbonate and cements from Sinemurian (lower Jurassic) siliceous sponge mounds (Djebel Bou Dahar, High Atlas, Morocco). *Chem. Geol.* 400, 65–86.
- Derry, L.A., Brasier, M.D., Corfield, R.M., Rozanov, A.Y., Zhuravlev, A.Y., 1994. Sr and C isotopes in lower Cambrian carbonates from the Siberian craton: a paleoenvironmental record during the ‘Cambrian explosion’. *Earth Planet. Sci. Lett.* 128, 671–681.
- Dodd, M.S., Zhang, Z., Li, C., Algeo, T.J., Lyons, T.W., Hardisty, D.S., Loyd, S.J., Meyer, D.L., Gill, B.C., Shi, W., Wang, W., 2021. Development of carbonate-associated phosphate (CAP) as a proxy for reconstructing ancient ocean phosphate levels. *Geochim. Cosmochim. Acta* 301, 48–69.
- Falcone, E.E., Federico, C., Boudoire, G., 2022. Geochemistry of trace metals and rare Earth elements in shallow marine water affected by hydrothermal fluids at Vulcano (Aeolian Islands, Italy). *Chem. Geol.* 593, 120756.
- Fan, T., Yu, K., Zhao, J., Jiang, W., Xu, S., Zhang, Y., Wang, R., Wang, Y., Feng, Y., Bian, L., Qian, H., Liao, W., 2020. Strontium isotope stratigraphy and paleomagnetic age constraints on the evolution history of coral reef islands, northern South China Sea. *GSA Bull.* 132, 803–816.
- Frimmel, H.E., 2009. Trace element distribution in Neoproterozoic carbonates as palaeoenvironmental indicator. *Chem. Geol.* 258, 338–353.
- German, C.R., Elderfield, H., 1990. Application of the Ce anomaly as a paleoredox indicator: the ground rules. *Paleoceanography* 5, 823–833.
- Gong, S.-Y., Li, H.-C., Siringan, F.P., Zhao, M., Kang, S.-C., Chou, C.-Y., 2017. AMS Carbon-14 dating of microbial carbonates in Holocene coral reefs, Western Luzon, Philippines. *Quat. Int.* 447, 27–34.
- Heindel, K., Birgel, D., Brunner, B., Thiel, V., Westphal, H., Gischler, E., Ziegenbalg, S.B., Cabioch, G., Sjövall, P., Peckmann, J., 2012. Post-glacial microbialite formation in coral reefs of the Pacific, Atlantic, and Indian Oceans. *Chem. Geol.* 304–305, 117–130.
- Higgins, J.A., Blättler, C.L., Lundstrom, E.A., Santiago-Ramos, D.P., Akhtar, A.A., Crüger Ahm, A.S., Bialik, O., Holmden, C., Bradbury, H., Murray, S.T., Swart, P.K., 2018. Mineralogy, early marine diagenesis, and the chemistry of shallow-water carbonate sediments. *Geochim. Cosmochim. Acta* 220, 512–534.
- Jia, Y., Wu, H., Yan, W., Zhang, C., Hu, B., Zhang, J., Tian, L., Deng, C., 2024. Rare earth element geochemistry of reef carbonates in the South China Sea since the Miocene: Insights into paleoclimatic significance. *J. Asian Earth Sci.* 265, 106094.
- Jiang, W., Yu, K.F., Song, Y.X., Zhao, J.X., Feng, Y.X., Wang, Y.H., Xu, S.D., 2017. Coral trace metal of natural and anthropogenic influences in the northern South China Sea. *Sci. Total Environ.* 607–608, 195–203.
- Jiang, W., Yu, K., Fan, T., Xu, S., Wang, R., Zhang, Y., Yue, Y., Zhao, J.-X., Feng, Y.-X., Wei, C., Wang, S., Wang, Y., 2019. Coral reef carbonate record of the Pliocene-Pleistocene climate transition from an atoll in the South China Sea. *Mar. Geol.* 411, 88–97.

- Kamber, B.S., Webb, G.E., 2001. The geochemistry of late Archaean microbial carbonate: implications for ocean chemistry and continental erosion history. *Geochim. Cosmochim. Acta* 65, 2509–2525.
- Kamber, B.S., Webb, G.E., Gallagher, M., 2014. The rare earth element signal in Archaean microbial carbonate: information on ocean redox and biogenicity. *J. Geol. Soc. Lond.* 171, 745–763.
- Kaufman, A.J., Knoll, A.H., 1995. Neoproterozoic variations in the C-isotopic composition of seawater: stratigraphic and biogeochemical implications. *Precambrian Res.* 73, 27–49.
- Lakshatanov, L., Stipp, S., 2004. Experimental study of europium (III) coprecipitation with calcite. *Geochim. Cosmochim. Acta* 68, 819–827.
- Li, G., Xu, W., Luo, Y., Liu, J., Zhao, J., Feng, Y., Cheng, J., Sun, Z., Xiang, R., Xu, M., Yan, W., 2023. Strontium isotope stratigraphy and LA-ICP-MS U-Pb carbonate age constraints on the Cenozoic tectonic evolution of the southern South China Sea. *GSA Bull.* 135, 271–285.
- Li, R., Jones, B., 2014. Evaluation of carbonate diagenesis: a comparative study of minor elements, trace elements, and rare-earth elements (REE+Y) between Pleistocene corals and matrices from Grand Cayman, British West Indies. *Sediment. Geol.* 314, 31–46.
- Li, X., Liu, Y., Wu, C.-C., Sun, R., Zheng, L., Lone, M.A., Shen, C.-C., 2019. Coral-inferred monsoon and biologically driven fractionation of offshore seawater rare earth elements in Beibu Gulf, northern South China Sea. *Solid Earth Sci.* 4, 131–141.
- Liu, X., Fan, H., Zhang, H., Xiao, C., Yang, H., Zhou, T., Tang, Y., Shang, P., Zhu, C., Wen, H., 2023. The REY geochemistry of phosphorites during metamorphism of the Haizhou Group, NW Yangtze Block, China. *Chem. Geol.* 641, 121781.
- Liu, X.-F., Zhai, S., Wang, X.-K., Liu, X., Liu, X.-M., 2022. Rare Earth Element Geochemistry of late Cenozoic Island Carbonates in the South China Sea. *Minerals* 12, 578.
- Luo, Y., Li, G., Xu, W., Liu, J., Cheng, J., Zhao, J., Yan, W., 2021. The effect of diagenesis on rare earth element geochemistry of the Quaternary carbonates at an isolated coral atoll in the South China Sea. *Sediment. Geol.* 420, 105933.
- Ma, Y., Qin, Y., Yu, K., Li, Y., Long, Y., Wang, R., Fan, T., Jiang, W., Xu, S., Zhao, J., 2021. Holocene coral reef development in Changhai Island, Northern South China Sea, and its record of sea level changes. *Mar. Geol.* 440, 106593.
- MacNeil, A., Jones, B., 2003. Dolomitization of the Pedro Castle Formation (Pliocene), Cayman Brac, British West Indies. *Sediment. Geol.* 162, 219–238.
- Mazumdar, A., Tanaka, K., Takahashi, T., Kawabe, I., 2003. Characteristics of rare earth element abundances in shallow marine continental platform carbonates of late Neoproterozoic successions from India. *Geochem. J.* 37, 277–289.
- McLennan, S., 1989. Rare earth elements in sedimentary rocks; influence of provenance and sedimentary processes. *Rev. Mineral. Geochem.* 21, 169–200.
- Monbet, P., Brunskill, G.J., Zagorskis, I., Pfitzner, J., 2007. Phosphorus speciation in the sediment and mass balance for the central region of the Great Barrier Reef continental shelf (Australia). *Geochim. Cosmochim. Acta* 71, 2762–2779.
- Nguyen, A.D., Zhao, J.X., Feng, Y.X., Hu, W.P., Yu, K.F., Gasparon, M., Pham, T.B., Clark, T.R., 2013. Impact of recent coastal development and human activities on Nha Trang Bay, Vietnam: evidence from a *Porites lutea* geochemical record. *Coral Reefs* 32, 181–193.
- Ning, Z., Fang, C., Yu, K., Yang, B., Dan, S.F., Xia, R., Jiang, Y., Li, R., Wang, Y., 2020. Influences of phosphorus concentration and porewater advection on phosphorus dynamics in carbonate sands around the Weizhou Island, northern South China Sea. *Mar. Pollut. Bull.* 160, 111668.
- Nothdurft, L.D., Webb, G.E., Kamber, B.S., 2004. Rare earth element geochemistry of late Devonian reefal carbonates, Canning Basin, Western Australia: confirmation of a seawater REE proxy in ancient limestones. *Geochim. Cosmochim. Acta* 68, 263–283.
- Nozaki, Y., Zhang, J., Amakawa, H., 1997. The fractionation between Y and Ho in the marine environment. *Earth Planet. Sci. Lett.* 148, 329–340.
- Olivier, N., Boyet, M., 2006. Rare earth and trace elements of microbialites in Upper Jurassic coral- and sponge-microbialite reefs. *Chem. Geol.* 230, 105–123.
- Qin, Y., Yu, K., Wang, R., Jiang, W., Xu, S., 2019. The initiation time of the holocene coral reef at the Changhai island (Xisha islands) and its significance as a sea level indicator. *Trop. Geogr.* 39, 319–328.
- Reynard, B., Lécuyer, C., Grandjean, P., 1999. Crystal-chemical controls on rare-earth element concentrations in fossil biogenic apatites and implications for paleoenvironmental reconstructions. *Chem. Geol.* 155, 233–241.
- Saha, N., Rodriguez-Ramirez, A., Nguyen, A.D., Clark, T.R., Zhao, J.-X., Webb, G.E., 2018. Seasonal to decadal scale influence of environmental drivers on Ba/Ca and Y/Ca in coral aragonite from the southern Great Barrier Reef. *Sci. Total Environ.* 639, 1099–1109.
- Saha, N., Webb, G.E., Zhao, J.-X., Duc Nguyen, A., Lewis, S.E., Lough, J.M., 2019. Coral-based high-resolution rare earth element proxy for terrestrial sediment discharge affecting coastal seawater quality, Great Barrier Reef. *Geochim. Cosmochim. Acta* 254, 173–191.
- Saha, N., Webb, G.E., Zhao, J.-X., Lewis, S.E., Duc Nguyen, A., Feng, Y., 2021. Spatiotemporal variation of rare earth elements from river to reef continuum aids monitoring of terrigenous sources in the Great Barrier Reef. *Geochim. Cosmochim. Acta* 299, 85–112.
- Salas-Saavedra, M., Webb, G.E., Sanborn, K.L., Zhao, J.-X., Webster, J.M., Nothdurft, L. D., Nguyen, A., 2022. Holocene microbialite geochemistry records > 6000 years of secular influence of terrigenous flux on water quality for the southern Great Barrier Reef. *Chem. Geol.* 604, 120871.
- Scherer, M., Seitz, H., 1980. Rare-earth element distribution in Holocene and Pleistocene corals and their redistribution during diagenesis. *Chem. Geol.* 28, 279–289.
- Shao, L., Li, Q., Zhu, W., Zhang, D., Qiao, P., Liu, X., You, L., Cui, Y., Dong, X., 2017. Neogene carbonate platform development in the NW South China Sea: Litho-, bio- and chemo-stratigraphic evidence. *Mar. Geol.* 385, 233–243.
- Shen, J., Wang, Y., 2008. Modern microbialites and their environmental significance, Meiji reef atoll, Nansha (Spratly) Islands, South China Sea. *Sci. China Ser. D-Earth Sci.* 51, 608–617.
- Shen, R., Shen, A., Yu, K., McCormick, C.A., Jiang, W., Xiao, Y., Wu, L., Wang, R., 2023. Properties of dolomitizing fluids indicated by rare earth elements: a case study of the Upper Miocene to Pliocene dolostone on the Xisha Islands, South China Sea. *Sediment. Geol.* 455, 106475.
- Sholkovitz, E., Shen, G.T., 1995. The incorporation of rare earth elements in modern coral. *Geochim. Cosmochim. Acta* 59, 2749–2756.
- Stipp, S., Lakshatanov, L., Jensen, J., Baker, J., 2003. Eu 3+ uptake by calcite: preliminary results from coprecipitation experiments and observations with surface-sensitive techniques. *J. Contam. Hydrol.* 61, 33–43.
- Tanaka, K., Kawabe, I., 2006. REE abundances in ancient seawater inferred from marine limestone and experimental REE partition coefficients between calcite and aqueous solution. *Geochem. J.* 40, 425–435.
- Tanaka, K., Miura, N., Asahara, Y., Kawabe, I., 2003. Rare earth element and strontium isotopic study of seamount-type limestones in Mesozoic accretionary complex of Southern Chichibu Terrane, Central Japan: Implication for incorporation process of seawater REE into limestones. *Geochem. J.* 37, 163–180.
- Teng, J., Shen, J., 2008. Microbial carbonates in Holocene beachrocks, Shuiweiling, Luhuitou Peninsula, Hainan Island. *Sci. China Ser. D-Earth Sci.* 51, 30–40.
- Terakado, Y., Masuda, A., 1988. The coprecipitation of rare-earth elements with calcite and aragonite. *Chem. Geol.* 69, 103–110.
- Tostevin, R., Shields, G.A., Tarbuck, G.M., He, T., Clarkson, M.O., Wood, R.A., 2016. Effective use of cerium anomalies as a redox proxy in carbonate-dominated marine settings. *Chem. Geol.* 438, 146–162.
- Toyama, K., Terakado, Y., 2019. Estimation of the practical partition coefficients of rare earth elements between limestone and seawater: Discussion and application. *Geochem. J.* 53, 139–150.
- Webb, G.E., Jell, J.S., 2006. Growth rate of Holocene reefal microbialites? Implications for use as environmental proxies, Heron Reef southern Great Barrier Reef. *ASEG Extend. Abstrac.* 2006, 1–3.
- Webb, G.E., Kamber, B.S., 2000. Rare earth elements in Holocene reefal microbialites: a new shallow seawater proxy. *Geochim. Cosmochim. Acta* 64, 1557–1565.
- Webb, G.E., Nothdurft, L.D., Kamber, B.S., Klopogge, J.T., Zhao, J.-X., 2009. Rare earth element geochemistry of scleractinian coral skeleton during meteoric diagenesis: a sequence through neomorphism of aragonite to calcite. *Sedimentology* 56, 1433–1463.
- Wei, G.-Y., Zhang, F., 2024. Pristine or altered, what can early diagenesis tell us in shallow-water carbonates? *Earth Planet. Sci. Lett.* 641, 118806.
- Wei, G.-Y., Zhang, F., Yin, Y.-S., Lin, Y.-B., Pogge von Strandmann, P.A.E., Cao, M., Li, N., Xiong, G., Chen, X., Fan, C., Xu, C., Tan, F., Zhang, X., Yang, H., Ling, H.-F., Shen, S.-Z., 2023b. A 13 million-year record of Li isotope compositions in island carbonates: Constraints on bulk inorganic carbonate as a global seawater Li isotope archive. *Geochim. Cosmochim. Acta* 344, 59–72.
- Wei, H., Liu, G., Han, X., Zhao, Y., Wu, J., Yang, J., Li, S., Zhang, Y., Li, D., 2023a. Coral-based rare earth element proxy for hydrothermal fluid on the Yongxing Island, South China Sea. *Ore Geol. Rev.* 162, 105678.
- Westphal, H., Heindel, K., Brandano, M., Peckmann, J., 2010. Genesis of microbialites as contemporaneous framework components of deglacial coral reefs, Tahiti (IODP 310). *Facies* 56, 337–352.
- Wu, S., Yang, Z., Wang, D., Lü, F., Lüdmann, T., Fulthorpe, C., Wang, B., 2014. Architecture, development and geological control of the Xisha carbonate platforms, northwestern South China Sea. *Mar. Geol.* 350, 71–83.
- Wyndham, T., McCulloch, M., Fallon, S., Alibert, C., 2004. High-resolution coral records of rare earth elements in coastal seawater: biogeochemical cycling and a new environmental proxy. *Geochim. Cosmochim. Acta* 68, 2067–2080.
- Xie, S., Jiang, W., Sun, Y., Yu, K., Feng, C., Han, Y., Xiao, Y., Wei, C., 2023. Interannual variation and sources identification of heavy metals in seawater near shipping lanes: evidence from a coral record from the northern South China Sea. *Sci. Total Environ.* 854, 158755.
- Xu, S., Yu, K., Fan, T., Jiang, W., Wang, R., Zhang, Y., Yue, Y., Wang, S., 2019. Coral reef carbonate  $\delta^{13}C$  records from the northern South China Sea: a useful proxy for seawater  $\delta^{13}C$  and the carbon cycle over the past 1.8 Ma. *Glob. Planet. Chang.* 182, 103003.
- Yang, H.-Q., Zhang, X.-Y., Li, Y., Shi, Q., Tao, S.-C., Mu, X.-N., Wang, M.-Z., Liu, X.-J., Tan, F., Zhou, S.-N., Wang, G., 2023. Biogenetic peloidal micrites within coral skeletons cause geochemical anomalies in reef limestones, Zhongsha Atoll, South China Sea. *Palaeogeogr. Palaeoclimatol. Palaeoecol.* 610, 111337.
- Yu, K., 2012. Coral reefs in the South China Sea: their response to and records on past environmental changes. *Sci. China Earth Sci.* 55, 1217–1229.
- Zhang, K., Shields, G.A., 2022. Sedimentary Ce anomalies: Secular change and implications for paleoenvironmental evolution. *Earth Sci. Rev.* 229, 104015.
- Zhang, X.-Y., Li, Y., Sun, F.-L., Tan, F., Shi, Q., Yan, H.-Q., Wang, G., Yang, H.-Q., 2022. Insights into microbially mediated cementation in modern beachrock in the Xisha Islands, South China Sea. *Palaeogeogr. Palaeoclimatol. Palaeoecol.* 592, 110904.
- Zhao, H., Jones, B., 2013. Distribution and interpretation of rare earth elements and yttrium in Cenozoic dolostones and limestones on Cayman Brac, British West Indies. *Sediment. Geol.* 284–285, 26–38.
- Zhao, M.-Y., Zheng, Y.-F., 2014. Marine carbonate records of terrigenous input into Paleothethyan seawater: Geochemical constraints from Carboniferous limestones. *Geochim. Cosmochim. Acta* 141, 508–531.
- Zhao, Y., Wei, W., Li, S., Yang, T., Zhang, R., Somerville, I., Santosh, M., Wei, H., Wu, J., Yang, J., Chen, W., Tang, Z., 2021. Rare earth element geochemistry of carbonates as

a proxy for deep-time environmental reconstruction. *Palaeogeogr. Palaeoclimatol. Palaeoecol.* 574, 110443.

Zhao, Y., Wei, W., Santosh, M., Hu, J., Wei, H., Yang, J., Liu, S., Zhang, G., Yang, D., Li, S., 2022. A review of retrieving pristine rare earth element signatures from carbonates. *Palaeogeogr. Palaeoclimatol. Palaeoecol.* 586, 110765.

Zhong, S., Mucci, A., 1995. Partitioning of rare earth elements (REEs) between calcite and seawater solutions at 25 C and 1 atm, and high dissolved REE concentrations. *Geochim. Cosmochim. Acta* 59, 443–453.